Endoluminal MR Imaging of the Rectum and Anus: Technique, Applications, and Pitfalls[1]

Jaap Stoker, MD
Elena Rociu, MD
Andries W. Zwamborn
W. Ruud Schouten, MD
Johan S. Laméris, MD

Anorectal diseases (eg, fecal incontinence, perianal and anovaginal fistulas, anorectal tumors) require imaging for proper case management. Endoluminal magnetic resonance (MR) imaging has become an important part of diagnostic work-up in such cases. Optimal endoluminal MR imaging requires careful attention to patient preparation, imaging protocols, and potential pitfalls in interpretation. Comfortable positioning and the use of an antiperistaltic drug are vital for adequate patient preparation. Selected sequences and imaging planes are used in imaging protocols tailored for specific diseases. In fecal incontinence, three-dimensional sequences allow detailed demonstration of the anal anatomy and related defects. In perianal and anovaginal fistulas, longitudinal imaging planes help determine the superior extent of the abnormality. In anorectal tumors, T1-weighted turbo spin-echo MR imaging can help detect extension into the perirectal fat and T2-weighted turbo spin-echo MR imaging is used to optimize contrast between tumor and the rectal wall. Off-axis and radial imaging planes are used in all anorectal diseases to minimize partial volume effects. Potential pitfalls include various parts of the normal anal anatomy mimicking sphincter defects, veins and hemorrhoids mimicking fistulas and abscesses, and overhanging tumor mimicking more extensive tumor. Adequate patient preparation combined with proper technique and a knowledge of potential pitfalls will allow optimal endoluminal MR imaging of the rectum and anus.

Abbreviation: GRE = gradient echo

Index terms: Anus, MR, 757.121411, 757.121413 • Magnetic resonance (MR), intracavitary coils • Rectum, MR, 757.121411, 757.121413 • Rectum, neoplasms, 757.30

RadioGraphics 1999; 19:383–398

[1]From the Departments of Radiology (J.S., E.R., A.W.Z., J.S.L.) and Surgery (W.R.S.), University Hospital Rotterdam Dijkzigt, Erasmus University Rotterdam, the Netherlands, and the Department of Radiology, Academic Medical Center, P.O. Box 22700, 1100 DE Amsterdam, the Netherlands (J.S., J.S.L.). Recipient of a Certificate of Merit award for a scientific exhibit at the 1997 RSNA scientific assembly. Received March 26, 1998; revision requested April 27 and received June 12; accepted June 15. **Address reprint requests to** J.S.

■ INTRODUCTION

Magnetic resonance (MR) imaging has become a valuable tool in the diagnostic work-up of patients with anorectal disease. Endoluminal MR imaging combines the high contrast resolution inherent in MR imaging with the high spatial resolution of an endoluminal coil. In this article, we discuss and illustrate endoluminal MR imaging of the rectum and anus, evaluate possible applications, and demonstrate potential pitfalls and limitations associated with this technique. Particular emphasis is placed on fecal incontinence, perianal and anovaginal fistulas, and anorectal tumors.

■ ENDOLUMINAL MR IMAGING TECHNIQUE

● Imaging Coils and Patient Preparation

The type of coil used for endoluminal MR imaging depends on the MR imager. For endoluminal MR imaging of the rectum, a coil with a balloon is commonly used (Fig 1). This coil gives satisfactory results in the imaging of rectal diseases but is not designed for endoanal imaging. However, dedicated endoluminal coils for the rectum and anus have also been developed (1–5). Two types of coils are currently in use. One is a cylindric saddle-geometry receiver coil, which ranges from 6 to 10 cm in length and from 7 to 12 mm in diameter (2,4,6,7). The coil is placed in a rigid, thin protective cover and immobilized with an external clamp. We use a rectangular, receive-only coil 8 cm long and 17 mm in diameter (1,3,5,8–13). The coil is surrounded by a rigid cylindric coil holder 10 cm long and 19 mm in diameter (Fig 1). The coil holder is 2 cm longer at the handgrip side of the coil to prevent expulsion by anal squeezing. Because the coil has no balloon and no external point of attachment, the angulation of the coil can easily be adjusted for optimal patient comfort. The position of the coil must be secured by placing small sandbags on the part of the coil outside the patient.

Patient preparation is part of every MR imaging procedure. The aim of patient preparation is to familiarize the patient with the procedure, to make the procedure as comfortable as possible, and to stress the importance of minimizing motion. The presence of an endoluminal coil may induce motion in the form of anal squeezing or pelvic floor contraction. Nevertheless, minimizing motion during image acquisition is especially important with endoluminal MR imaging, which involves the use of small voxels and is therefore more susceptible to image degradation by motion.

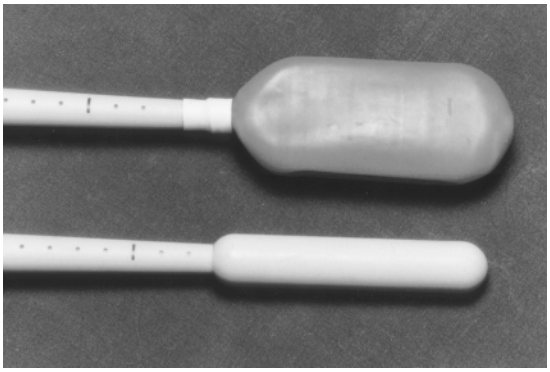

Figure 1. Photograph shows endoluminal coils for endorectal (top) and endoanal (bottom) MR imaging.

Patients with anorectal tumors undergo an enema to clean the rectum prior to examination. All patients are asked to void to prevent motion artifacts that may result from discomfort caused by a distended bladder. A rectal digital examination is performed only in patients with rectal tumors to determine tumor location and optimal coil positioning. The endoluminal coil is covered with a condom, and a small amount of lubricant is applied to the top of the coil. Excessive lubrication should be avoided because it may cause very high signal intensity next to the coil and lead to near field effect, a phenomenon that is common with standard surface coils and can also occur with an endoluminal surface coil. Near field effect describes the large differences in signal intensity caused by the high sensitivity close to the coil and the steep drop-off in sensitivity as distance from the coil increases.

The endoanal coil is introduced with the patient in the left lateral decubitus position. The patient then turns to the supine position, the coil position is checked, and the coil is secured with sandbags. Patient comfort is enhanced with use of a small pillow positioned over the coil and sandbags and a fixation band around the legs. The patient is instructed not to squeeze during the imaging procedure and to relax the pelvic floor and related muscles as much as possible.

Sagittal scout images are obtained, followed by off-axis coronal and axial scout images obtained parallel and orthogonal to the coil, respectively. The coil position is reevaluated, and the coil is repositioned if necessary. Once optimal coil position is achieved, 20 mg of butylscopalamine bromide (Buscopan; Boehringer,

Ingelheim, Germany) or 1 mg of glucagon is injected intramuscularly. This is important for both rectal and anal imaging because it helps reduce motion artifacts caused by rectal contractions.

• Imaging Sequences

The optimal imaging sequences for endoluminal MR imaging of the rectum and anus have not yet been determined. T1-weighted MR imaging with intravenously administered contrast material, short-inversion-time inversion recovery imaging, and T2-weighted spin-echo MR imaging have all been advocated (2,4,7). In our experience, proton-density–weighted gradient-echo (GRE) and T2-weighted turbo spin-echo MR imaging give optimal results without contrast enhancement. Proton-density–weighted and T2-weighted MR imaging sequences clearly demonstrate normal anal anatomy and anal disease (1,3,5,8) and are, therefore, the mainstays of our imaging protocols for endoluminal MR imaging of the rectum and anus. In patients with fecal incontinence, detailed demonstration of the anal sphincter anatomy is essential. Three-dimensional proton-density–weighted GRE MR imaging provides the requisite high spatial resolution. Of greater importance in patients with anovaginal and especially perianal fistulas is the higher contrast resolution of T2-weighted turbo spin-echo MR imaging, which facilitates identification of even small amounts of fluid or thin, inflamed walls. In subtle cases, fat suppression techniques (fat saturation, spectral inversion recovery, short-inversion-time inversion recovery) might help increase the level of confidence and is therefore included in our imaging protocol for perianal fistulas. Contrast enhancement might be useful in the detection of perianal fistulas; to our knowledge, however, no study has demonstrated the superiority of contrast-enhanced imaging over other types of imaging. Anovaginal fistulas are most easily identified against the background of hyperintense veins in the anovaginal septum; consequently, imaging sequences with which veins appear hyperintense (eg, T2-weighted, GRE, and contrast-enhanced T1-weighted sequences) should be used. In patients with anorectal tumors, tumor-wall contrast is optimal on T2-weighted turbo spin-echo MR images. Proton-density–weighted GRE MR images are too susceptible to motion artifacts caused by rectal contractions. Characterization of tumor extension through the wall into the perirectal fat or anal sphincter and identification of enlarged lymph nodes are best achieved with T1-weighted imaging. The use of intravenously administered contrast material can help determine tumor extent, and the use of dynamic MR imaging (eg, TurboFLASH; Siemens Medical Systems, Iselin, NJ) has been advocated to improve differentiation between T2 and T3 tumor.

Despite the use of butylscopalamine bromide or glucagon, some motion artifacts often occur in the phase-encoding direction due to rectal contractions. The phase-encoding direction is left to right in patients with fecal incontinence and anovaginal fistulas because disease is expected anteriorly. In perianal fistulas, there is no clear preference for the phase-encoding direction; the external opening might be an indicator, but often the tract has no clear-cut superoinferior dimension. In anorectal tumors, findings at rectal digital examination can indicate the preferred phase-encoding direction; in most cases, however, part of the tumor will lie in the phase-encoding direction.

• Imaging Planes

All imaging planes used for endoluminal MR imaging are off-axis planes oriented orthogonal or parallel to the coil and anorectum, thereby facilitating identification of normal anorectal anatomy and related diseases and reducing partial volume effects. The axial plane is optimal in the evaluation of anorectal disease. Use of one or more longitudinal sequences allows better appreciation of the superoinferior extent of disease (9). Coronal and sagittal sequences or a radial sequence may be used. The sections of a radial sequence are not parallel but oriented like the spokes of a wheel. The signal void at the center of the sequence corresponds to the signal void at the center of the coil and will not interfere with imaging. A radial sequence has the theoretical advantage that all sections are perpendicular to the coil and anorectum, resulting in fewer partial volume effects. More important, this sequence is more time efficient than a coronal or sagittal sequence (9). The interpretation of anal anatomy is somewhat more difficult with a radial sequence; consequently, coronal and sagittal sequences are the preferred longitudinal sequences in patients with fecal incontinence. Perianal fistulas and anorectal tumors can be evaluated with axial and radial T2-weighted turbo spin-echo MR imaging. This is especially advantageous in anorectal tumors because it leads to fewer partial volume effects. In anovaginal fistulas, axial and sagittal sequences are the most informative because they demonstrate the tract with an anteroposterior orientation.

Table 1
Imaging Sequences for Endoluminal MR Imaging

Sequence	Repetition Time (msec)	Echo Time (msec)	Flip Angle (degrees)	Section Width (mm)*	Field of View	Matrix	Echo Train Length	No. of Signals Averaged
Proton-density–weighted gradient echo†	23.7	13.8	60	2 (0)	112 × 140	256 × 256	…	2
T2-weighted turbo spin echo‡	2,500	100	90	3 (0.3)	90 × 160	253 × 512	10	3
T1-weighted turbo spin echo	500	17	90	3 (0.3)	135 × 180	255 × 512	5	4

* Numbers in parentheses indicate gap between sections (in millimeters).
† Should be performed first because of susceptibility to motion artifacts.
‡ Can be combined with fat-suppression sequences (spectral inversion recovery, fat saturation) for perianal fistulas, or short-inversion-time inversion recovery turbo spin-echo sequences may be used.

Table 2
Imaging Protocols for Endoluminal MR Imaging

Pathologic Condition	Imaging Plane	Sequence	Scan Time (min)	Procedure Time (min)
Fecal incontinence	Axial	Proton-density–weighted gradient echo	16	40
	Coronal	T2-weighted turbo spin echo		
	Sagittal	T2-weighted turbo spin echo		
Perianal fistula	Axial	T2-weighted turbo spin echo	17	45
	Axial	T2-weighted turbo spin echo*		
	Radial	T2-weighted turbo spin echo		
Anovaginal fistula	Axial	T2-weighted turbo spin echo	10	30
	Sagittal	T2-weighted turbo spin echo		
Anorectal tumor†	Axial	T2-weighted turbo spin echo	21	50
	Axial	T1-weighted turbo spin echo		
	Radial	T2-weighted turbo spin echo		
	Radial	T1-weighted turbo spin echo‡		

* Sequence performed with fat suppression (spectral inversion recovery, fat saturation).
† Additional sequences for detection of liver metastases and iliac lymph nodes should be performed with a body coil or array coil.
‡ Sequence performed with intravenously administered contrast material.

● Imaging Protocols

The imaging sequences and protocols used at our institution for endoluminal MR imaging of the rectum and anus at 1.5 T (Gyroscan ACS-NT; Philips Medical Systems, Best, the Netherlands) are shown in Tables 1 and 2.

■ NORMAL ANAL SPHINCTER ANATOMY

Controversy exists concerning normal anal sphincter anatomy. Present understanding is based on the results of anatomic dissection and surgery. The discussion focuses on whether the external sphincter comprises several parts and whether the puborectal muscle is an important component of the sphincter complex.

The advantage of endoluminal MR imaging over anatomic dissection and surgery lies in its multiplanar capability, which is of paramount importance for understanding the anatomy of the anal sphincter and related structures. The relationship between the external sphincter and the puborectal muscle is especially appreciated at endoluminal MR imaging (1): The external sphincter is the outer part of the lower half of the anal sphincter, and the puborectal muscle is the outer part of the upper half of the sphincter (Fig 2). The fat-containing ischioanal space surrounds the anal sphincter complex (Fig 2). Endoanal MR imaging findings concerning the internal sphincter, intersphincteric space, and longitudinal muscle are in approximate agreement with previous data. The internal sphincter

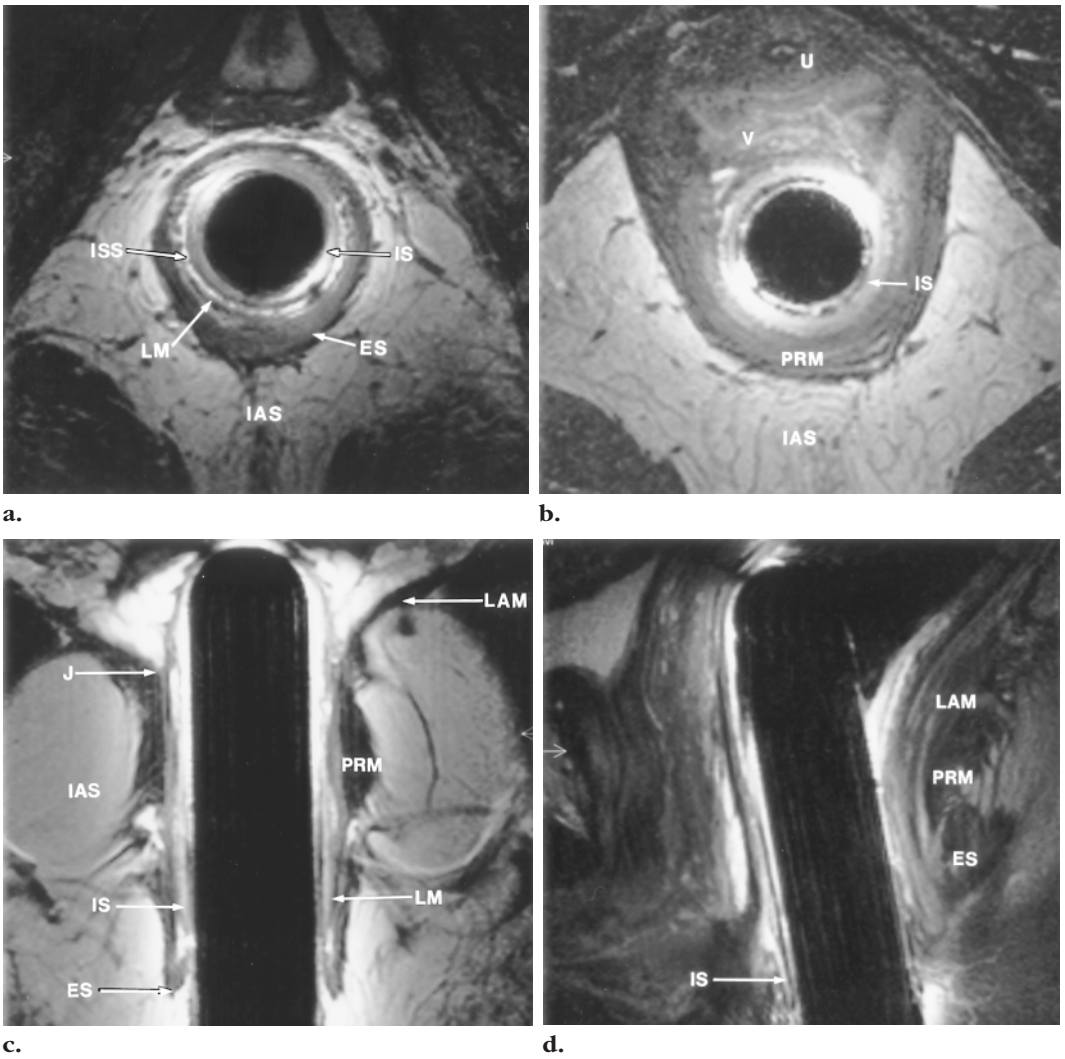

Figure 2. **(a)** Axial proton-density–weighted GRE (repetition time msec/echo time msec = 23.7/13.8) MR image through the lower part of the anal sphincter shows the external sphincter (*ES*) as the outer part of the sphincter complex and as relatively hypointense. The internal sphincter (*IS*) is the inner muscular part of the sphincter complex and is relatively hyperintense. The longitudinal muscle (*LM*) is within the intersphincteric space (*ISS*) between the internal and external sphincters. The sphincter complex is surrounded by the ischioanal space (*IAS*). **(b)** Axial proton-density–weighted GRE (23.7/13.8) MR image through the upper part of the sphincter complex shows the slinglike puborectal muscle (*PRM*) as the outer part of the complex. The muscle is relatively hypointense. *IAS* = ischioanal space, *IS* = internal sphincter, *U* = urethra, *V* = vagina. **(c)** Coronal T2-weighted turbo spin-echo (2,500/100) MR image through the anal sphincter clearly demonstrates the muscular parts of the anal sphincter and their relation to each other. *ES* = external sphincter, *IAS* = ischioanal space, *IS* = internal sphincter, *J* = anorectal junction, *LAM* = levator ani muscle, *LM* = longitudinal muscle, *PRM* = puborectal muscle. **(d)** Midsagittal T2-weighted turbo spin-echo (2,500/100) MR image through the anal sphincter clearly demonstrates the relation between the external sphincter (*ES*) and the puborectal muscle (*PRM*), especially posteriorly. *IS* = internal sphincter, *LAM* = levator ani muscle.

is the continuation of the circular muscle of the rectum and is the inner part of the anal sphincter (Fig 2). The internal sphincter is surrounded by the fat-containing intersphincteric space, which is in turn surrounded by the external sphincter (Fig 2a). Within the intersphincteric space is the longitudinal muscle, which is the continuation of the longitudinal muscle of the rectum (Fig 2a).

■ FECAL INCONTINENCE

Fecal incontinence is an important medical and social problem. Approximately 2% of persons over 45 years of age suffer from this disease (10). Anal sphincter defects are a major cause of fecal incontinence. These defects are often the

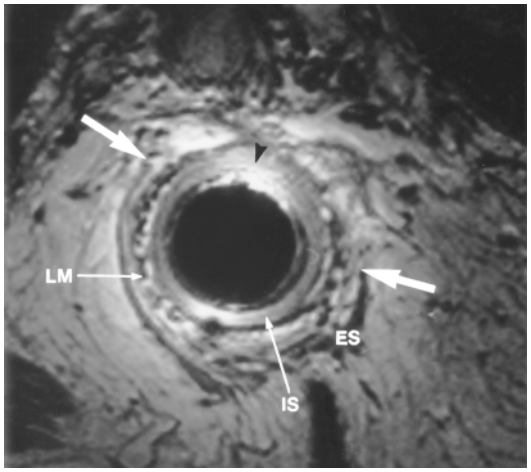

3.

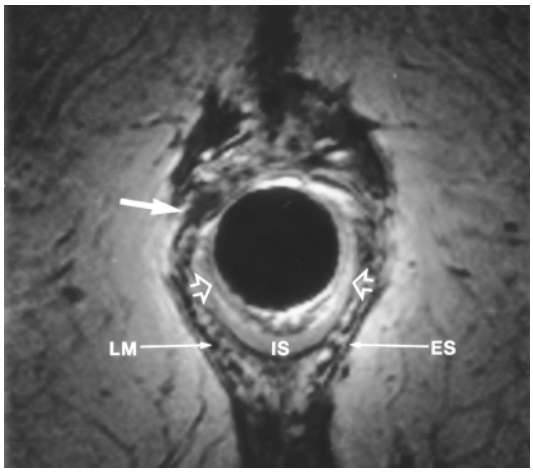

4.

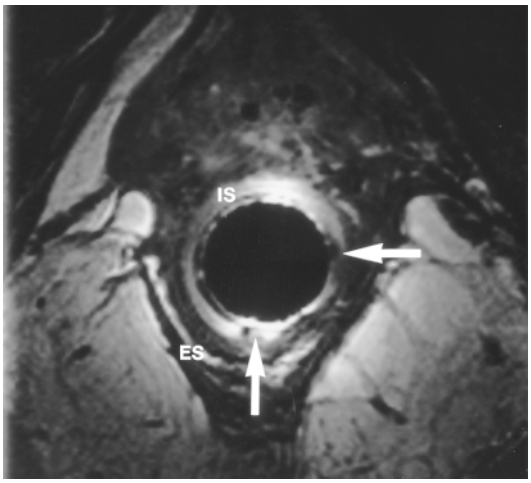

5a.

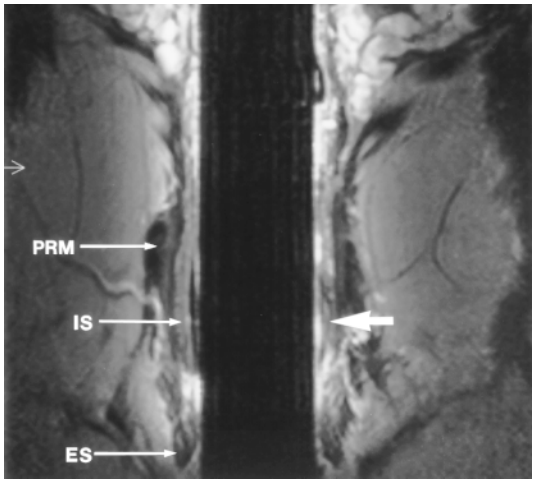

5b.

Figures 3–5. **(3)** Axial proton-density–weighted GRE (23.7/13.8) MR image shows a large anterior defect (arrows) of the external sphincter (*ES*), which is somewhat atrophic. A relatively small lesion (arrowhead) is seen in the left anterior aspect of the internal sphincter (*IS*). *LM* = longitudinal muscle. **(4)** Axial proton-density–weighted GRE (23.7/13.8) MR image shows an anterior defect (open arrows) of the internal sphincter (*IS*). An anterior defect and scar tissue (solid arrow) of the longitudinal muscle (*LM*) and external sphincter (*ES*) are also seen. **(5a)** Axial proton-density–weighted GRE (23.7/13.8) MR image demonstrates a left-sided posterolateral defect and scar tissue (arrows) of the internal sphincter (*IS*). Compare the normal right lateral aspect of the internal sphincter. The left posterolateral aspect of the external sphincter (*ES*) is somewhat irregular. **(5b)** Coronal T2-weighted turbo spin-echo (2,500/100) MR image helps confirm the findings in **a**. Compare the normal right aspect of the internal sphincter (*IS*) with the lesion on the left (arrow). The superoinferior extent of the lesion is clearly evident. *ES* = external sphincter, *PRM* = puborectal muscle.

result of vaginal delivery or anal surgery. Less commonly, they may be caused by a deficient sphincter after surgery for anal atresia or trauma. Anal sphincter defects can be clinically occult.

In patients with fecal incontinence, imaging can be used to identify and characterize anal sphincter defects. Most defects are located in the anterior part of the external and internal sphincter because vaginal delivery is the major cause of fecal incontinence.

Only endoluminal MR imaging can demonstrate the anal anatomy in sufficient detail. Recent studies indicate that anal sphincter anatomy and sphincter lesions are better demonstrated with endoluminal MR imaging than with endoanal sonography (1–4,6–8,11,12). Besides defects, other forms of sphincter damage (eg, scar tissue) may also be encountered (Figs 3–7). Endoluminal MR imaging is the only imaging technique that can demonstrate atrophy of the external sphincter (Fig 8). External sphincter atrophy consists of a diffuse thinning of the external sphincter muscle or replacement of muscle by

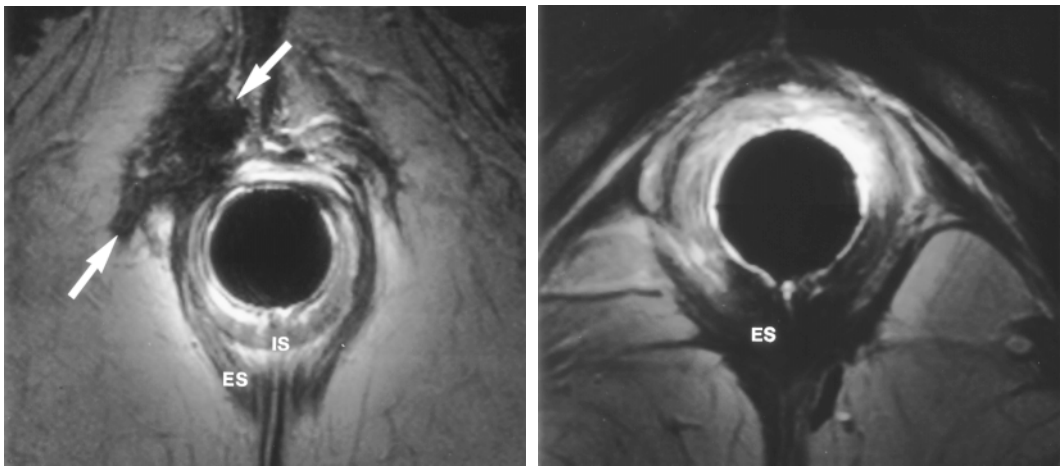

6. 7.

Figures 6, 7. **(6)** Axial T2-weighted turbo spin-echo (2,500/100) MR image of the lower part of the anal sphincter reveals scar tissue (arrows) outside the right lateral aspect of the external sphincter (*ES*). The scar tissue resulted from a right-sided lateral episiotomy. *IS* = internal sphincter. **(7)** Axial T2-weighted turbo spin-echo (2,500/100) MR image obtained after surgery for anal atresia reveals an absent internal sphincter and an anteriorly deficient external sphincter (*ES*) bilaterally.

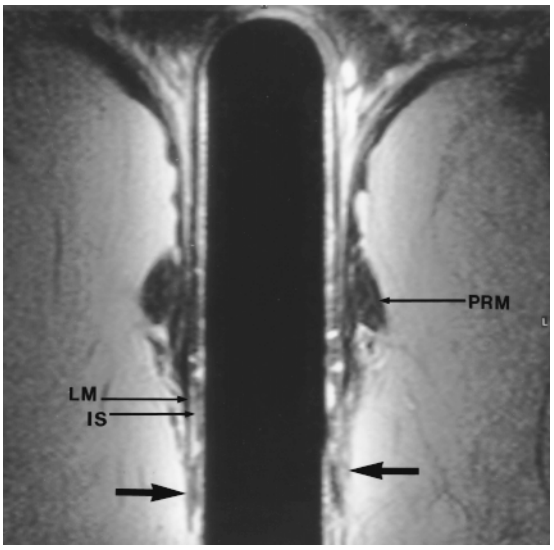

Figure 8. Coronal T2-weighted turbo spin-echo (2,500/100) MR image shows an atrophic external sphincter, only some thin portions of which remain (arrows) (cf Fig 2c). The internal sphincter (*IS*), longitudinal muscle (*LM*), and puborectal muscle (*PRM*) are normal.

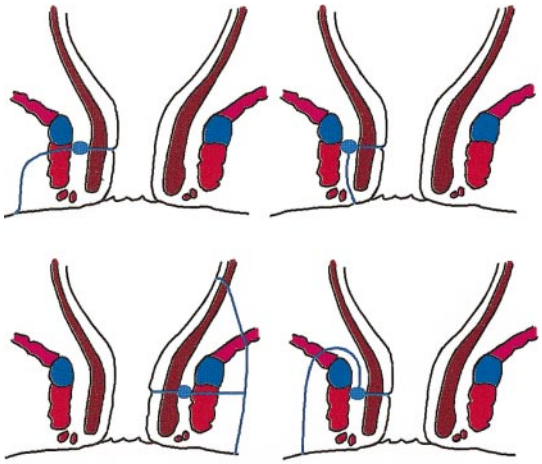

Figure 9. Illustration shows Parks classification of perianal fistulas. There is a transsphincteric fistula with extension of the tract through the external sphincter (upper left), an intersphincteric tract confined to the intersphincteric space and internal sphincter (upper right), a fistula passing through the levator ani muscle over the top of the puborectalis muscle into the intersphincteric space (suprasphincteric fistula) (lower right), and an extrasphincteric fistula passing through the ischiorectal fossa and levator ani muscle into the rectum (lower left).

fat. A recent study showed that external sphincter atrophy is an important predictor of negative outcome for anterior anal repair of anal sphincter defects (13).

■ PERIANAL AND ANOVAGINAL FISTULAS

Perianal fistulas and anovaginal fistulas have different causes (inflammation versus trauma), resulting in different manifestations at MR imaging. Anovaginal fistulas are thin walled and have little or no fluid or air in the tract. Perianal fistulas often have a relatively thick fibrous wall, are fluid filled, and enhance after intravenous administration of contrast material. Nonactive perianal tracts are fibrous bands without fluid or significant enhancement. Perianal fistulas are classified for proper surgical therapy (Figs 9–16) (14). The presence (Fig 13) or absence

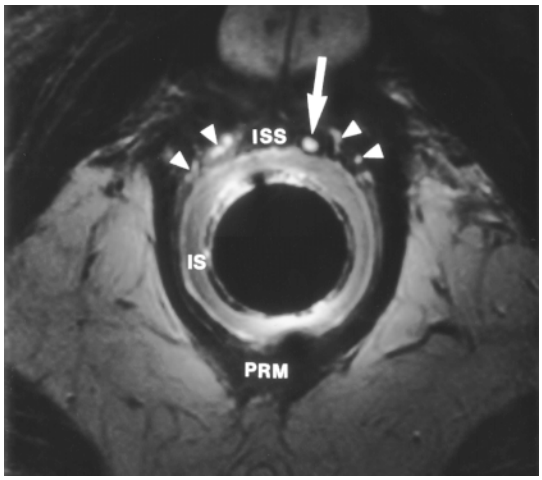

10a.

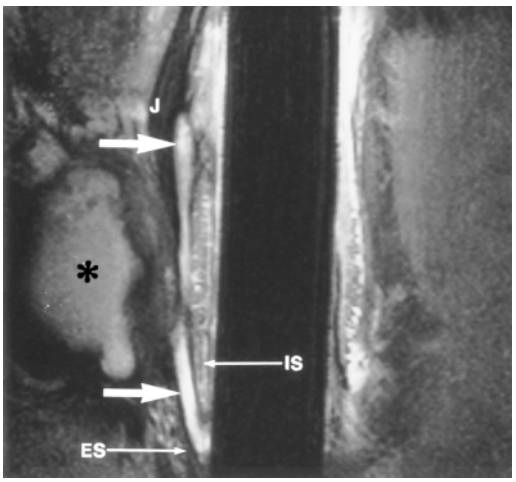

10b.

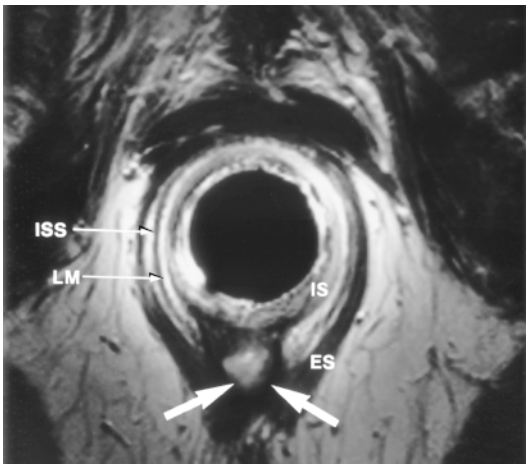

11a.

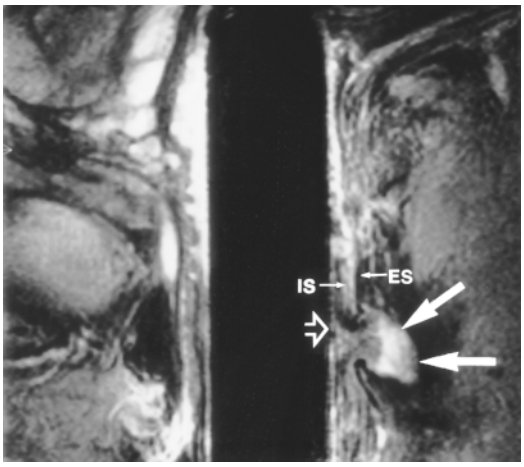

11b.

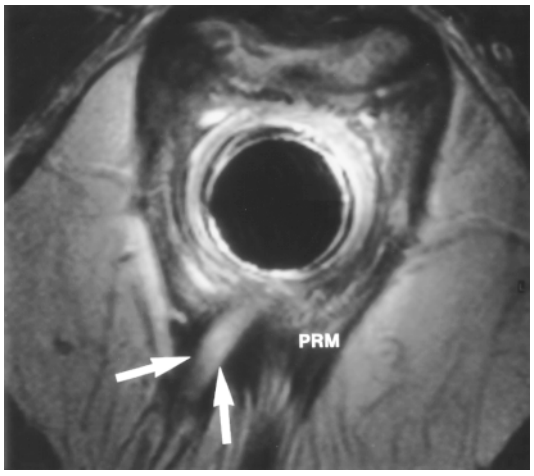

12a.

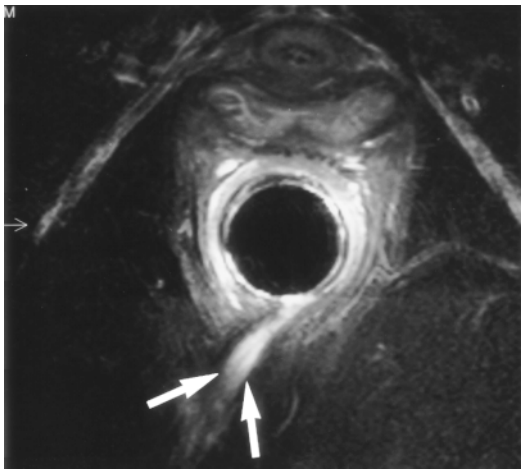

12b.

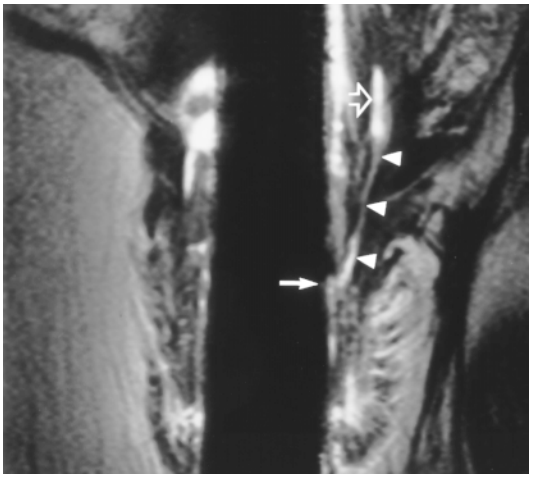

13.

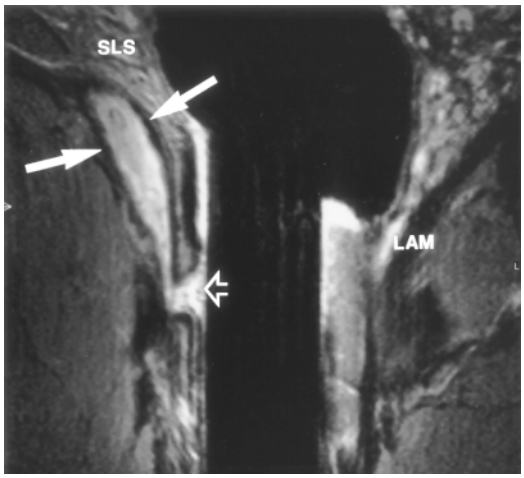

14.

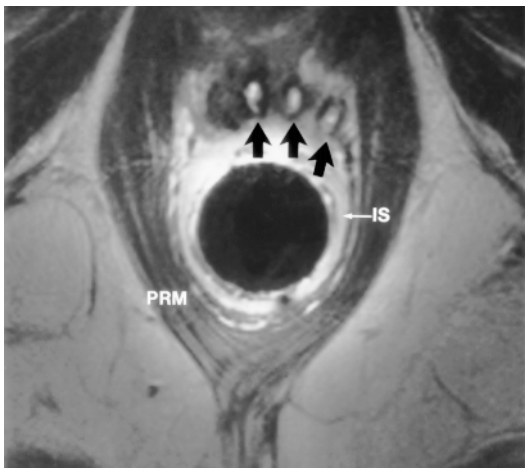

15.

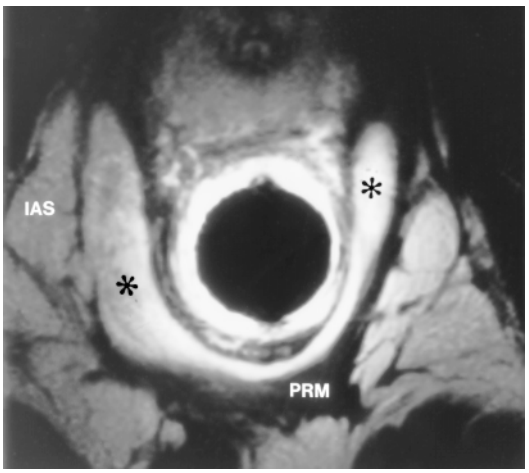

16.

Figures 13–16. **(13)** Coronal T2-weighted turbo spin-echo (2,500/100) MR image demonstrates a supralevatoric abscess (open arrow) with a tract (arrowheads) and an infralevatoric internal opening (solid arrow). **(14)** Radial oblique T2-weighted turbo spin-echo (2,500/100) MR image shows an abscess (solid arrows) in the levator ani muscle (*LAM*) but no extension into the supralevator space (*SLS*). The internal opening of the abscess (open arrow) is clearly visible. **(15)** Axial T2-weighted turbo spin-echo (2,500/100) MR image of the upper part of the anal sphincter in a patient suspected of having a complex fistula shows multiple tracts anteriorly (arrows). *IS* = internal sphincter, *PRM* = puborectal muscle. **(16)** Axial T2-weighted turbo spin-echo (2,500/100) MR image through the upper part of the sphincter complex demonstrates a horseshoe-shaped abscess (*) in the puborectal muscle (*PRM*) and the ischioanal space (*IAS*).

Figures 10–12. **(10a)** Axial T2-weighted turbo spin-echo (2,500/100) MR image of the upper part of the anal sphincter demonstrates a fistula (arrow) in the intersphincteric space (*ISS*) anteriorly. Some veins are also seen anteriorly (arrowheads). *IS* = internal sphincter, *PRM* = puborectal muscle. **(10b)** Sagittal slightly oblique T2-weighted turbo spin-echo (2,500/100) MR image shows a tract (arrows) that is limited to the intersphincteric space between the internal sphincter (*IS*) and the external sphincter (*ES*) and is therefore classified as an intersphincteric fistula. The tract approaches the anorectal junction (*J*) but does not extend into the supralevator space. A cavernous body is seen anteriorly (*). **(11a)** Axial T2-weighted turbo spin-echo (2,500/100) MR image demonstrates an abscess (arrows) in the intersphincteric space (*ISS*) posteriorly. *ES* = external sphincter, *IS* = internal sphincter, *LM* = longitudinal muscle. **(11b)** Sagittal slightly oblique T2-weighted turbo spin-echo (2,500/100) MR image shows the internal opening (open arrow) of the intersphincteric abscess (solid arrows) and the relation of the fistula to the internal sphincter (*IS*) and external sphincter (*ES*). **(12a)** Axial T2-weighted turbo spin-echo (2,500/100) MR image of the upper part of the anal sphincter demonstrates a fistula (arrows) traversing the puborectal muscle (*PRM*) posteriorly on the right. The tract is classified as a transsphincteric fistula. This fistula has the typical morphology of an active perianal fistula in that the tract is filled with fluid. **(12b)** On an axial T2-weighted turbo spin-echo (2,500/100) MR image obtained with spectral inversion recovery (fat saturation), the tract is more conspicuous (arrows).

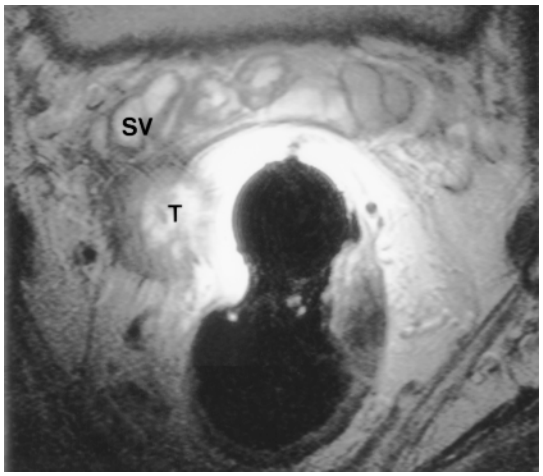

18. **19.**

Figures 18, 19. **(18)** Coronal radial oblique T2-weighted turbo spin-echo (2,500/100) MR image demonstrates a lobulated rectal tumor (*T*) extending close to the anorectal junction (*J*). There is no extension through the muscular layer (arrowhead) into the perirectal fat, and no enlarged lymph nodes are seen. *SV* = seminal vesicles. **(19)** Axial T2-weighted turbo spin-echo (2,500/100) MR image shows a recurrent rectal adenocarcinoma (*T*). The tumor has a spiculated border with invasion of the right seminal vesicle (*SV*). The window setting was optimized for demonstration of the tumor and seminal vesicle, resulting in high signal intensity near the imaging coil.

(Fig 14) of supralevator extent is important in planning surgical therapy. Fistulas may be complex with multiple tracts (Fig 15) and may have horseshoe-shaped abscesses (Fig 16). Recent studies have demonstrated that MR imaging is the preferred modality in perianal fistulas. Endoanal MR imaging is superior to endoanal sonography and body-coil MR imaging (3,5). Tracts can be identified with T2-weighted sequences, fat suppression techniques, or contrast-enhanced T1-weighted sequences. The usefulness of contrast enhancement is debatable. Contrast enhancement increases the cost of a procedure and, to our knowledge, has never been demonstrated to be superior to unenhanced techniques. The most important indicator for the presence of a tract or abscess is an abnormal longitudinal or oval structure with a fibrous wall and (often) fluid in the lumen in the anorectal region. Such a structure can be appreciated with T2-weighted sequences, fat suppression techniques, or contrast-enhanced T1-weighted sequences. Further study is needed to determine the optimal imaging sequence for perianal fistulas.

Limited data concerning imaging of anovaginal fistulas have been published. To our knowledge, no comparative data on endoluminal sonography, conventional MR imaging, or endoluminal MR imaging have been compiled. In our limited experience, endoluminal sonography and endoluminal MR imaging seem to produce comparable results (Fig 17).

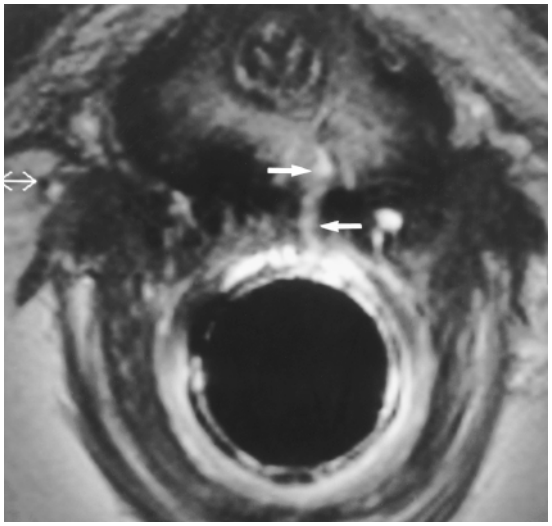

Figure 17. Axial T2-weighted turbo spin-echo (2,500/100) MR image in a woman with a clinical history of anovaginal fistula after vaginal delivery shows an anovaginal fistula filled with hyperintense fluid (arrows).

■ ANORECTAL TUMORS

Three important issues must be addressed in local staging of anorectal tumors: tumor invasion through the wall, lymph node enlargement, and distance between tumor and anorectal junction (Figs 18–21). At present, four imaging methods are commonly used for staging: endoluminal sonography, body-coil MR imaging, phased-array-coil MR imaging, and endoluminal MR imaging. Theoretically, endoluminal imaging will

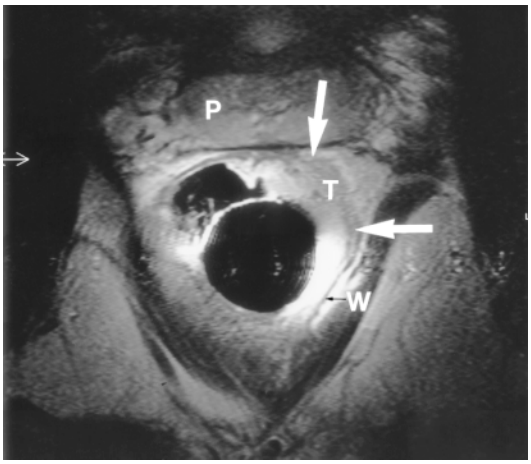

20a.

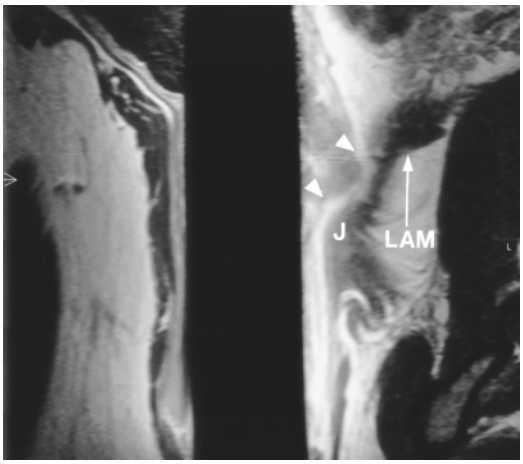

20b.

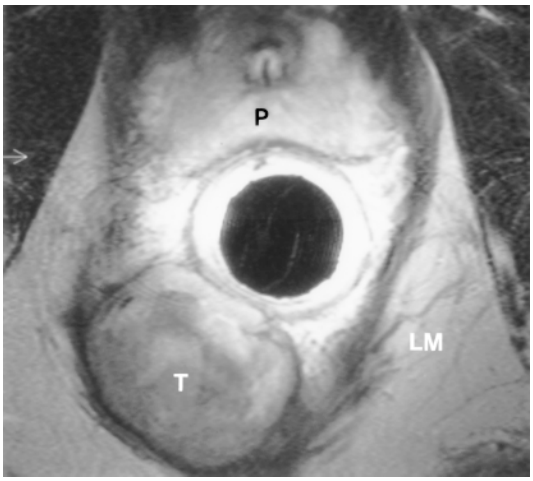

21a.

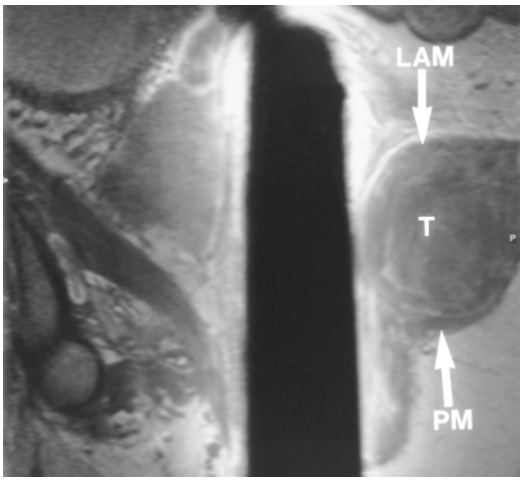

21b.

Figures 20, 21. **(20a)** Axial T2-weighted turbo spin-echo (2,500/100) MR image demonstrates invasion of a rectal tumor (*T*) through the rectal wall (*W*) into the perirectal fat (arrows). No invasion of the prostate gland (*P*) is seen. **(20b)** Coronal radial oblique T1-weighted turbo spin-echo (500/17) MR image obtained after administration of gadodiamide (Omniscan; Nycomed, Oslo, Norway) shows invasion of the perirectal fat (arrowheads). The tumor is seen displacing but not invading the levator ani muscle (*LAM*) and is very close to the anorectal junction (*J*). A fat plane is visible between the tumor and the levator ani muscle. **(21a)** Axial T2-weighted turbo spin-echo (2,500/100) MR image shows non-Hodgkin lymphoma (*T*) adjacent to the longitudinal muscle (*LM*). The exact tumor location is difficult to determine without a complementary longitudinal imaging sequence. *P* = prostate gland. **(21b)** Sagittal radial oblique T1-weighted turbo spin-echo (500/17) MR image obtained after administration of gadodiamide reveals that the tumor (*T*) is located between the puborectal muscle (*PM*) and the levator ani muscle (*LAM*).

yield optimal staging results because it combines the high spatial resolution of an endoluminal technique with the high contrast resolution intrinsic to MR imaging (15,16). The accuracy (75%–85%) of endoluminal MR imaging is superior to that of body-coil MR imaging, but whether this will lead to better surgical outcomes remains uncertain (17–19). A recent study demonstrated the importance of intravenous administration of contrast material for accurate staging (19). Limitations of endoluminal MR imaging and other imaging techniques include overstaging caused by desmoplastic reaction and understaging in cases of microscopic infiltration in or through the wall. Overstaging seems to occur more frequently. A recent study investigated the value of dynamic MR imaging (TurboFLASH) for differentiation between T2 and T3 tumor

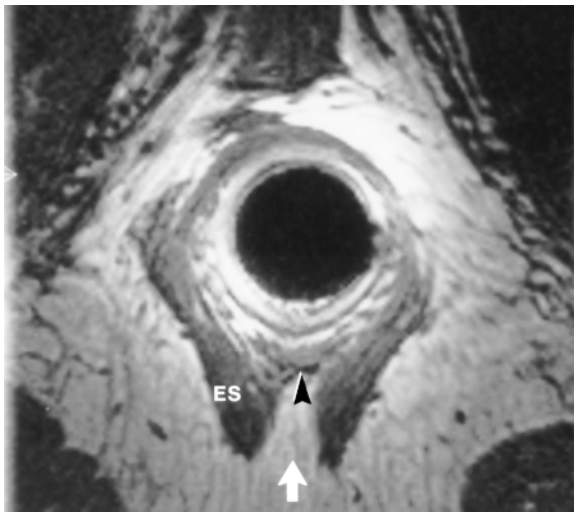

22.

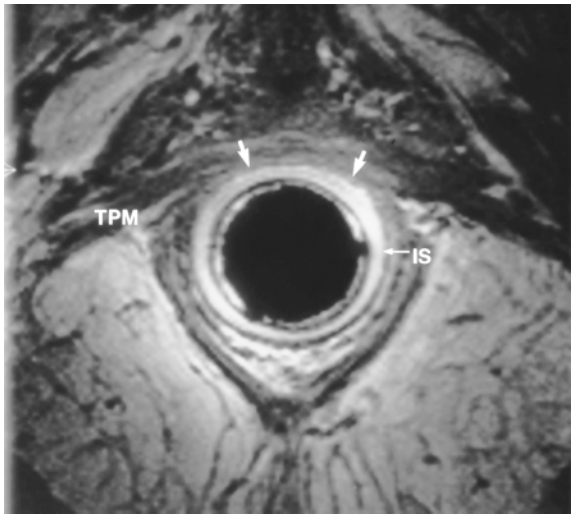

23.

Figures 22, 23. **(22)** On an axial proton-density–weighted GRE (23.7/13.8) MR image obtained 2.5 cm above the lower edge of the external sphincter in a male patient, the morphology of the external sphincter (*ES*) posteriorly (arrow) may suggest a tear but is actually a normal variant of the external sphincter. External sphincter tissue is also present more anteriorly (arrowhead). **(23)** Axial proton-density–weighted GRE (23.7/13.8) MR image obtained 1.4 cm superior to the caudal edge of the external sphincter in a female patient does not demonstrate the external sphincter anteriorly (arrows). This finding does not represent a defect but is the normal aspect of the anterior sphincter at this level in a female. The external sphincter is approximately 1.4–1.6 cm high in healthy females. *IS* = internal sphincter, *TPM* = transverse perineal muscle.

(19). Knowledge of the distance between tumor and anus is important in planning sphincter-saving surgery for rectal tumors (Fig 18). Endoluminal MR imaging may be more accurate than MR imaging with phased-array coils in very distal tumors because of its higher spatial resolution.

Both endoluminal and phased-array-coil MR imaging are limited in their ability to help detect lymph node metastases (18). Endoluminal MR imaging is clearly more accurate than the other available endoluminal technique, endoluminal sonography, in the staging of tumors or lymph nodes. For endoluminal MR imaging, the sensitivity is approximately 50%–80% (18). An endoluminal technique can help detect small lymph nodes close to the anorectum, but lymph nodes outside the field of view will be missed. This problem can be solved with use of additional body-coil or phased-array-coil sequences. None of the techniques mentioned allows reliable differentiation between reactive inflammatory lymph nodes and metastatic lymph nodes. Several attempts have been made to improve differentiation (eg, distinctions made on the basis of size and enhancement characteristics), but none has proved to be very accurate (19).

Comparative studies of rectal tumor staging are sparse and involve small study populations. In our experience, endoluminal MR imaging is preferable to endoluminal sonography because its multiplanar capability allows the distance between the tumor and the anorectal junction to be established more accurately. Data on phased-array-coil MR imaging are limited but indicate good results (20).

Further study is needed to establish the preferred technique for staging anorectal tumors.

■ PITFALLS

A variety of pitfalls are associated with endoluminal MR imaging, some of which are specific for the anorectal region. The wide variations in normal anal anatomy can lead to misinterpretation. The posterior part of the external sphincter can be partially open in males (Fig 22), a condition that can easily be recognized as a normal variant because of its symmetric aspect, smooth margins, and lack of scar tissue. More difficult to evaluate is the relatively short external sphincter seen anteriorly in females (Fig 23). Part of the anterior sphincter complex is supported by the transverse perineal muscle. This normal variant of the anterior anal sphincter might be misinterpreted as an anterior external sphincter defect. The relatively high sensitivity proximal to

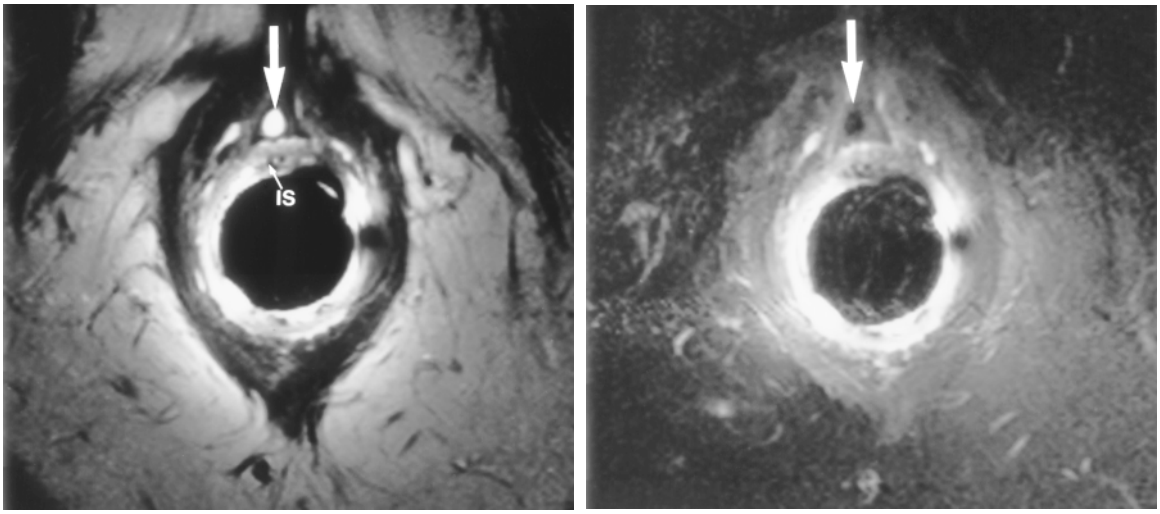

a. **b.**

Figure 24. **(a)** Axial T2-weighted turbo spin-echo (2,500/100) MR image of the central part of the anal sphincter in a patient with a complex fistula at the lower part of the sphincter shows a hyperintense oval structure (arrow) anterior to the internal sphincter (*IS*). This structure might be interpreted as a fistula or small abscess. The hyperintensity is caused by fat in the intersphincteric space, which also has high signal intensity due to high sensitivity proximal to the imaging coil (near field effect). **(b)** MR image obtained with spectral inversion recovery (fat saturation) shows the oval structure with low signal intensity (arrow).

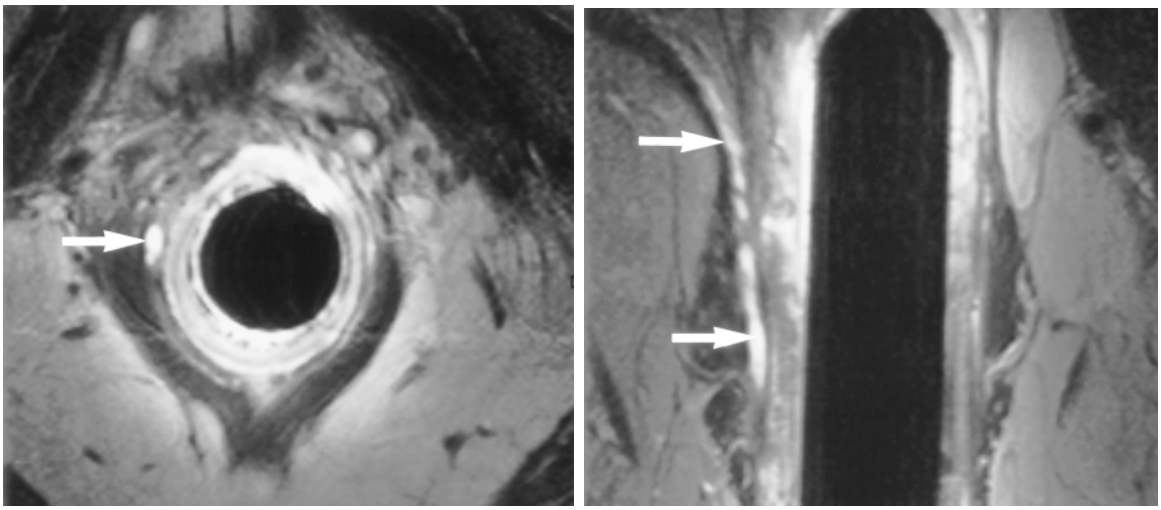

a. **b.**

Figure 25. **(a)** Axial T2-weighted turbo spin-echo (2,500/100) MR image shows a hyperintense structure (arrow) in the intersphincteric space that may represent a fistula. **(b)** On a coronal slightly oblique T2-weighted turbo spin-echo (2,500/100) MR image, the hyperintense structure in the right lateral aspect of the intersphincteric space (arrows) has a very thin wall and a lobulated, serpiginous aspect. This structure is a vein and not a fistula. The vein is continuous with the periprostatic veins. Compare this case with the perianal fistula shown in Figure 10b, which has a straighter course, a thicker wall, and no connection to vascular structures.

an endoluminal coil may cause fat to have very high signal intensity at T2-weighted turbo spin-echo MR imaging and to be misconstrued as a fistula or abscess (Fig 24). However, this potential pitfall can often be avoided by recognizing that other fat at a comparable distance from the coil also has high signal intensity. Fat suppression can be useful in equivocal cases (Fig 24b).

The venous anatomy of the anal sphincter region is complex, and multiple veins are present in the submucosal, intersphincteric, and ischioanal spaces. Although the veins are often identified correctly, a vein might be misinterpreted as a fistulous tract (Fig 25a). Both veins and fistulas

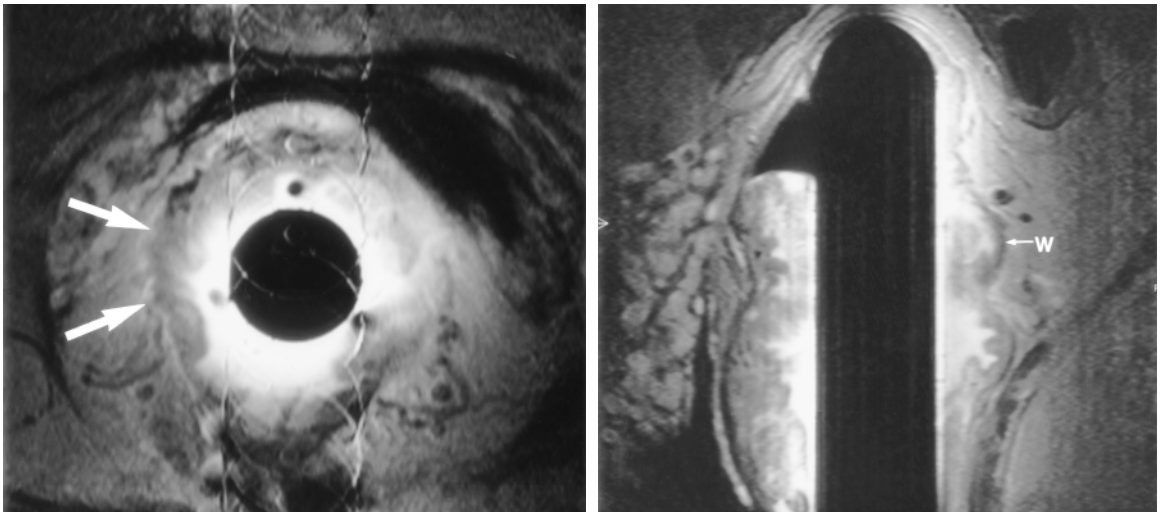

a. **b.**

Figure 26. **(a)** Axial T2-weighted turbo spin-echo (2,500/100) MR image of a patient with a rectal carcinoma demonstrates artifacts in the phase-encoding direction caused by rectal contractions. The MR imaging findings might be interpreted as tumor invasion through the rectal wall (arrows) because no normal muscular layer is visible. **(b)** Sagittal oblique T2-weighted turbo spin-echo (2,500/100) MR image reveals that there is no invasion in or through the muscular layer of the rectal wall (*W*). The partial volume effects seen in **a** are not present. This case demonstrates the importance of longitudinal sequences as part of the imaging protocol.

can be hyperintense on T2-weighted MR images and can enhance on contrast-enhanced images. Veins can be differentiated from fistulas in that veins have a tortuous course and thin walls and are continuous with other veins (Fig 25b). Fistulas are often characterized by a relatively straight course and thick fibrous walls and have an internal opening (Fig 10b). A hemorrhoid can be misinterpreted as an abscess. This pitfall can be avoided by recognizing that a hemorrhoid has a thin wall and is continuous with other venous structures.

The use of a single imaging plane may cause partial volume effects that can lead to incorrect staging in tumors (Fig 26). This pitfall can be avoided by including an additional plane in the imaging protocol. In distal rectal tumors, knowledge of the distance between tumor and anal sphincter is important in deciding whether to perform sphincter-saving surgery. Cauliflower-like tumors will overhang a part of the normal rectal wall, which can lead to underestimation of the tumor-sphincter distance (Fig 27). Such underestimation can be prevented by recognizing the cauliflower-like aspect of the tumor at digital rectal examination and identifying the base of the tumor at endoluminal MR imaging.

■ LIMITATIONS

About 10% of patients with perianal fistulas experience mild discomfort when the coil is introduced. Severe discomfort or anal stenosis prevents endoanal MR imaging in about 2% of patients with perianal fistulas. To our knowledge, no significant discomfort has been reported at coil introduction or during MR imaging in patients with fecal incontinence, anovaginal fistulas, or anorectal tumors.

The sensitive region of the endoluminal coil is large enough to allow evaluation of sphincter defects and anovaginal fistulas. Occasionally,

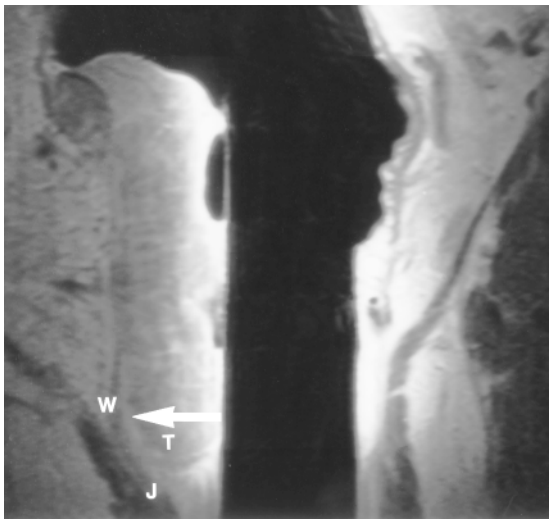

Figure 27. Coronal radial oblique T1-weighted turbo spin-echo (500/17) MR image obtained after administration of gadodiamide in a patient with a distal rectal tumor shows the tumor reaching nearly to the anorectal junction (*J*). However, high-signal-intensity inflammatory tissue (arrow) is visible between the overhanging lower part of the tumor (*T*) and the rectal wall (*W*). The tumor base is located 2 cm above the anorectal junction. Consequently, sphincter-saving surgery was performed. At surgery, the cauliflower-like tumor was seen to overhang the distal rectal wall. There was sufficient normal rectum distally to allow anastomosis.

large or high rectal tumors and extensive perianal fistulas may extend outside this region. In such cases, additional body-coil or phased-array-coil imaging sequences can be performed for complete visualization of the lesion. In long, tight strictures, the use of a body coil or phased-array coil is preferred; even in these patients, however, endoluminal MR imaging may allow correct staging. Endoluminal MR imaging can demonstrate enlarged perirectal lymph nodes, but body-coil or phased-array-coil MR imaging is necessary for the evaluation of parailiacal lymph nodes and liver.

■ CONCLUSIONS

Endoluminal MR imaging of the rectum and anus demonstrates anorectal anatomy and disease in considerable detail. Endoluminal MR imaging has significant advantages over other techniques such as endoluminal sonography and body-coil MR imaging, especially in the diagnostic work-up of patients with fecal incontinence and perianal fistulas. The superiority of endoluminal MR imaging in anovaginal fistulas and anorectal tumors is less well substantiated; to our knowledge, no studies have compared endoluminal MR imaging with phased-array-coil MR imaging in anovaginal fistulas. In our opinion, phased-array coils will provide adequate information in many patients with perianal fistulas and anorectal tumors. However, subtle abnormalities such as small blind tracts may go undetected. These tracts will give rise to recurrent perianal fistulas because colorectal surgeons will explore only preoperatively identified tracts to minimize sphincter damage. In fecal incontinence, endoluminal MR imaging is superior to phased-array-coil MR imaging, which demonstrates only limited anatomic detail. Distention of the anal sphincter by the endoluminal coil facilitates identification of sphincter defects because the edges of the defect are farther apart. Endoluminal MR imaging is an important technique in the diagnostic work-up of patients with anorectal disease. Adequate imaging techniques and protocols should be used, and one should be aware of specific pitfalls and limitations associated with this modality.

Acknowledgments: We thank Bert van Heerebeek, RT, for his help in optimizing the endoluminal MR imaging procedure and imaging protocols and Teun Rijsdijk for the high-quality photographs.

REFERENCES

1. Hussain SM, Stoker J, Laméris JS. Anal sphincter complex: endoanal MR imaging of normal anatomy. Radiology 1995; 197:671–677.
2. deSouza NM, Kmiot WA, Puni R, et al. High resolution magnetic resonance imaging of the anal sphincter using an internal coil. Gut 1995; 37:284–287.
3. Stoker J, Hussain SM, van Kempen D, Elevelt AJ, Laméris JS. Endoanal coil in MR imaging of anal fistulas. AJR 1996; 166:360–362.
4. deSouza NM, Hall AS, Puni R, Gilderdale DJ, Young IR, Kmiot WA. High resolution magnetic resonance imaging of the anal sphincter using a dedicated endoanal coil: comparison of magnetic resonance imaging with surgical findings. Dis Colon Rectum 1996; 39:926–934.
5. Hussain SM, Stoker J, Schouten WR, Laméris JS. Fistula in ano: endoanal sonography versus endoanal MR imaging in classification. Radiology 1996; 200:475–481.
6. deSouza NM, Puni R, Kmiot WA, Bartram CI, Hall AS, Bydder GM. MRI of the anal sphincter. J Comput Assist Tomogr 1995; 19:745–751.
7. deSouza NM, Gilderdale DJ, MacIver DK, Ward HC. High resolution MR imaging of the anal sphincter in children: a pilot study using endoanal receiver coils. AJR 1997; 169:201–206.
8. Hussain SM, Stoker J, Schütte HE, Laméris JS. Imaging the anorectal region. Eur J Radiol 1996; 22:116–122.
9. Stoker J, Jong Tjien Fa VE, Eijkemans MJC, Schouten WR, Laméris JS. Endoanal MR imaging of perianal fistulas: the optimal imaging planes. Eur Radiol 1998; 8:1212–1216.
10. Gordon PH, Nivatvongs S. Principles and practice of surgery of the colon, rectum and anus. St Louis, Mo: Quality Medical, 1992.
11. Stoker J, Hussain SM, Laméris JS. Endoanal magnetic resonance imaging versus sonography. Radiol Med 1996; 92:738–741.
12. Rociu E, Stoker J, Eijkemans MJC, Schouten WR, Laméris JS. Endoanal sonography versus endoanal MR imaging in fecal incontinence. Radiology (in press).
13. Rociu E, Stoker J, Briel JW, Hop WCJ, Schouten WR, Laméris JS. Endoanal MR imaging evaluation of sphincter atrophy (abstr). Radiology 1997; 205(P):453.
14. Parks AG, Gordon PH, Hardcastle JD. A classification of fistulo-in-ano. Br J Surg 1976; 63:1–12.
15. Chan TW, Kressel HY, Milestone B, et al. Rectal carcinoma: staging at MR imaging with endorectal surface coil. Radiology 1991; 181:461–467.
16. Schnall MD, Furth EE, Rosato EF, Kressel HY. Rectal tumor stage: correlation of endorectal MR imaging and pathologic findings. Radiology 1994; 190:709–714.
17. de Lange EE. Staging rectal carcinoma with endorectal imaging: how much detail do we really need? Radiology 1994; 190:633–635.
18. Blomqvist L, Holm T, Rubio C, Hindmarsh T. Rectal tumours: MR imaging with endorectal and/or phased array coils, and histopathological staging on giant sections—a comparative study. Acta Radiol 1997; 38:437–444.
19. Vogl TJ, Pegios W, Mack MG, et al. Accuracy of staging rectal tumors with contrast-enhanced transrectal MR imaging. AJR 1997; 168:1427–1434.
20. Brown G, Richards CJ, Williams GT, et al. Evaluation of thin slice MR imaging in the local staging of rectal cancer (abstr). Radiology 1997; 205(P):453.